*Progress In Electromagnetics Research, PIER 66, 157–171, 2006*

# PERFORMANCE APPRAISAL OF ACTIVE PHASED ARRAY ANTENNA IN PRESENCE OF A MULTILAYER FLAT SANDWICH RADOME

**A. Kedar, K. S. Beenamole, and U. K. Revankar**

Electronics & Radar Development Establishment
C.V. Raman Nagar, Bangalore-560093, India

**Abstract**—This paper studies the performance appraisal of radiation performance of ultra low sidelobe level Active Phased Array Antennas in presence of Multilayer Flat Sandwich Radome. Further, the effect of errors introduced due to amplitude/phase quantisation and planarity of the array surface, on the radiation performance has been studied. Based on these errors, manufacturing tolerances of the Flat Sandwich Radome have been suggested to control the deterioration of radiation performance within tolerable limits. This work is expected to be useful in development/manufacturing of radomes for Active Phased Array Radars and similar applications where ultra low sidelobe levels are required to be maintained.

## 1. INTRODUCTION

A Radar designer visualises the array antenna as a component with measurable input/output and a set of specifications. The array designer gets details of the array along with the physical and electrical limitations imposed by the radar, and within those constraints seeks to optimise the design. Radar has to discriminate between the targets and the clutter by using variety of discriminating and filtering techniques, requiring ultra low sidelobe level (SLL) Active Phased Array Antenna systems [1]. Hence, a radar antenna array protected by a low performance radome will be rendered useless, as radome deteriorates the radiation pattern drastically [1, 2].

Active Phased Array Antennas consist of stationary antenna elements, having variable excitation control at each element for pattern shaping and to electronically scan a beam to given angles in space. A variety of errors, both random and spatially correlated, introduced

across the array result in the degradation of radiation pattern [3–7]. The present paper discusses the effect of one of such prominent errors, i.e., quantised phase or amplitude errors caused by discrete phase shifters and discretised amplitude taper across the array.

The present paper briefs the study carried out on the effect of discretisation of amplitudes and phases, along with the effect of non-uniformity in the planarity of the array surface (array planarity), on the pattern performance of active phased array antenna. Further, study of degradation in radiation performance of active phased array antenna in presence of multilayer flat sandwich radome, including previously mentioned errors has been presented. Finally, manufacturing tolerance limits on multilayer flat sandwich radome have been suggested to control the array pattern distortion within tolerable limits.

## 2. THEORETICAL FORMULATION

The array factor (AF) for a $(M \times N)$ elements planar array antenna can be written as [5]:

$$F(u,v) = \sum_{m=1}^{M/2} \sum_{n=1}^{N/2} A_{mn} \cos[(m-0.5)kd_x u] \cos[(n-0.5)kd_y v]$$

$$u = \sin\theta\cos\phi - \sin\theta_0\cos\phi_0; \quad v = \sin\theta\sin\phi - \sin\theta_0\sin\phi_0 \tag{1}$$

$$A_{mn} = S(m,n)\exp(j\varphi_{mn}) \tag{2}$$

In (1), $\theta_0$ and $\phi_0$ are the beam pointing angles and in (2), $S(m,n)$ and (mn are the amplitude and phase values for the mnth array element placed at the location $(m,n)$ in the array grid [coordinate system is shown as an inset in Figure 1].

Further, the array is assumed to have an amplitude error, $\delta_{mn}$ and phase error, $\Phi_{mn}$ at the $mn$th element. Amplitude error $\delta_{mn}$ means that the signal at the $mn$th element has amplitude $(1+\delta_{mn})\ S_{mn}$, where $S_{mn}$ is the correct amplitude and phase error $\phi_{mn}$ implies that the correct phase to steer a beam to the chosen angle is $\exp(j\Phi_{mn})$ times the correct excitation. Incorporating these errors in AF, (2) is modified as

$$\begin{aligned} A_{mn} &= (1+\delta_{mn})S(m,n)\exp j(\Omega_{mn}) \\ \Omega_{mn} &= \phi_{mn} + \Phi_{mn} \end{aligned} \tag{3}$$

In the present paper, for reference a $(160 \times 10)$ elements planar array having interelement spacings in Azimuth and Elevation Planes as $d_x = 0.5\lambda_0$ and $d_y = 0.8\lambda_0$, respectively has been chosen, the resultant array aperture being $80\lambda_0 \times 8\lambda_0$ ($\lambda_0$ being the free space wavelength).

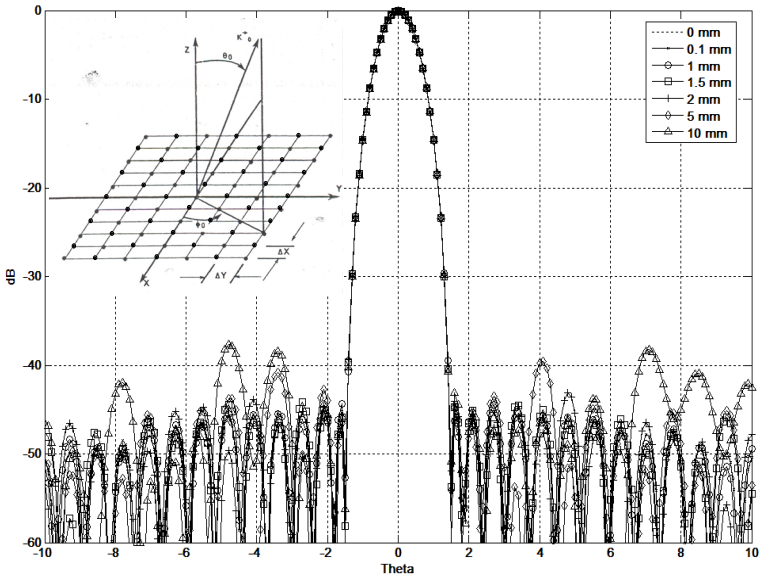


**Figure 1.** Effect of variation in array planarity (peak value) of (160 × 10) elements active phased array antenna on its far-field radiation pattern.

The array excitations are as per Taylor's $\overline{n}$ line distribution [5] for SLL of $-45$ dB and $-30$ dB in Azimuth and Elevation Planes, respectively. In the analysis, 6 bit quantisation of amplitude and phase excitations has been employed.

### 2.1. Effect of Array Planarity on the Active Phased Array Antenna Performance

Array Planarity (AP) refers to amount of non-uniformity in the surface planarity of the antenna array due to the involved manufacturing process, which may introduce some phase distortions leading to array pattern degradation. The magnitude of phase distortion ($\Lambda$) can be obtained from the following expression as:

$$\Lambda \text{ (in degrees)} = \frac{360}{\lambda_0} AP \tag{4}$$

While analysing the effect of array planarity on the radiation pattern of the active phased array antenna, $\Lambda$ may be introduced in the progressive phase shifts, in a random fashion as

$$\Omega_{mn} = \phi_{mn} + \Lambda \times r_{mn} \tag{5}$$

In (5), $\phi_{mn}$ corresponds to phase shift corresponding to $mn$th element, $\{r_{mn}\}$ is a sequence of random numbers between 0 and 1. Table 1 shows the magnitude of phase distortion, $\Lambda$ (at centre frequency, $f_0 = 3.3\,\text{GHz}$) corresponding to different values of array planarity ranging from $\pm 0.25\,\text{mm}$ (0.5 mm peak) to $\pm 5\,\text{mm}$ (10 mm peak). It has been shown that phase distortion is directly proportional to the magnitude of array planarity. Further, estimation of degradation in SLL has been made using (1)–(5), showing a direct relationship between SLL degradation and increase in array planarity [Figure 1]. The typical values of degradation in peak SLL (w.r.t. $-45\,\text{dB}$ SLL as reference) have been tabulated in Table 1. Hence, it can be concluded that array planarity should not deteriorate beyond certain limit so as to contain the array pattern distortion within desirable SLL limits.

**Table 1.** Variation in phase distortion (peak) and peak SLL degradation w.r.t. array planarity tolerance.

| Tolerance (Peak) (mm) | Phase Distortion ($\Lambda$) (Deg) | Peak SLL Degradation (dB) |
|---|---|---|
| 0.1 | 0.396 | 0.1 |
| 1 | 3.96 | 0.6 |
| 1.5 | 5.94 | 1.8 |
| 2 | 7.92 | 2.1 |
| 5 | 19.8 | 4.7 |
| 10 | 39.6 | 6.1 |

### 2.2. Effect of Quantisation Errors on the Active Phased Array Antenna Performance

In Active Phased Array Antennas, use of digital attenuators and phase shifters is preferred from practical point of view. These have fixed quantised levels, resulting in the periodic phase or amplitude errors across the array as if the array is constructed of subarrays with the quantised state defined for each subarray. These errors are highly correlated, resulting in large, well-defined sidelobe or grating-lobe-type peaks in the array pattern, called *quantisation lobes* [5, 7]. It has been shown that this discretisation allows only a staircase approximation of the continuous progressive shift required for the array, resulting in a periodic triangular phase error producing quantisation lobes [6]. Quantisation lobes deteriorate the radiation pattern of the antenna array in terms of gain, SLL and beam pointing accuracy.

The first quantisation lobe level for $n$-bit phase quantisation can

be estimated as $-6n$ dB [6]. The quantisation lobe level can often be reduced by disrupting the total periodicity leading to the large grating lobes [5–7]. Decreasing the step size or increasing the number of steps between the minimum (0°) and maximum (360°) values, can reduce the quantisation lobe level. This implies increase in the number of attenuators and phase shifter bits. However, increase in number of bits increases the cost and complexity of the system affecting the beam steering time. Hence the choice of bits is very important.

Out of the several methods proposed for reducing the quantisation lobe level, Two Probable Value Method [8] reduces the SLL to $-12n$ dB, for large $n$. This method has been used in the present study to reduce the quantisation lobe level introduced in the radiation pattern of active phased array antenna, and has been discussed in detail in our earlier work [9]. The effect of 6 bit amplitude and phase quantisation on array performance, clearly exhibiting degradation in SLL has been shown in Figures 2 and 3. Further, it can be clearly observed that the quantisation lobe level reduces due to the optimisation using Two Probable Value Method [Figure 3]. Figure 4 shows the combined effect of the 6 bit amplitude and phase quantisation (optimised using Two Probable Value Method) on the array performance. The radiation pattern has further deteriorated

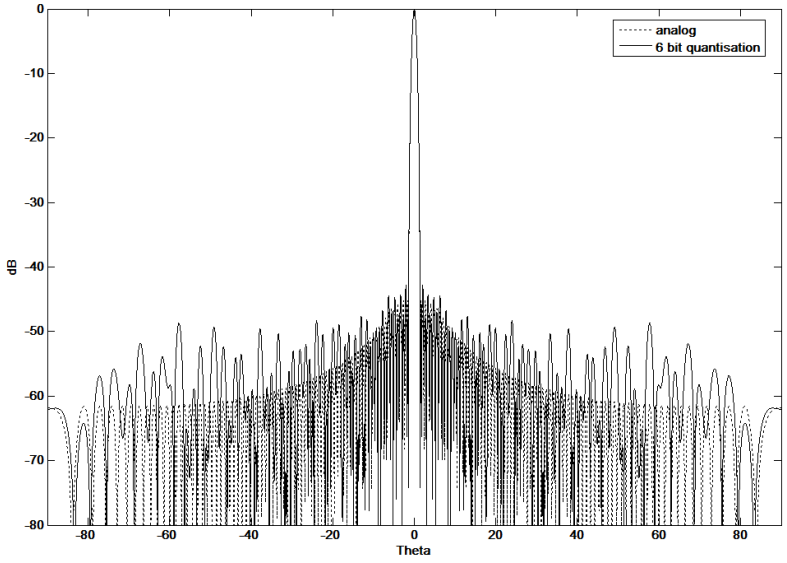


**Figure 2.** Effect of 6 bit amplitude quantisation on far-field radiation pattern of $(160 \times 10)$ elements active phased array antenna.

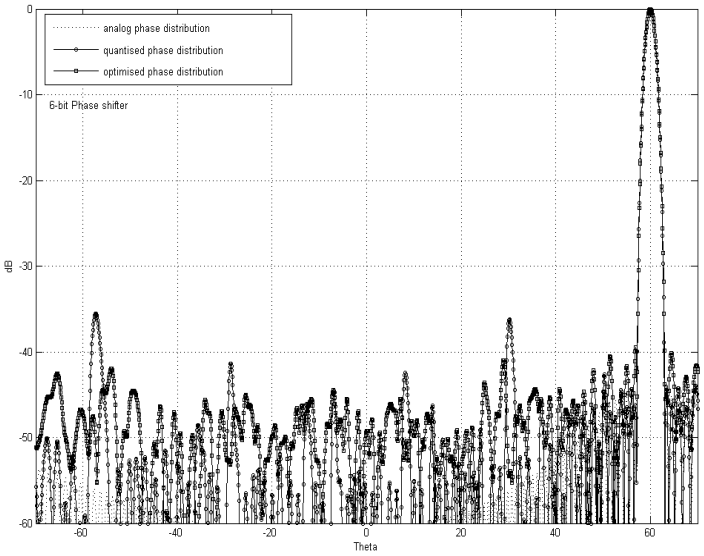


**Figure 3.** Effect of 6 bit phase quantisation with and without optimisation on far-field radiation pattern of $(160 \times 10)$ elements active phased array antenna.

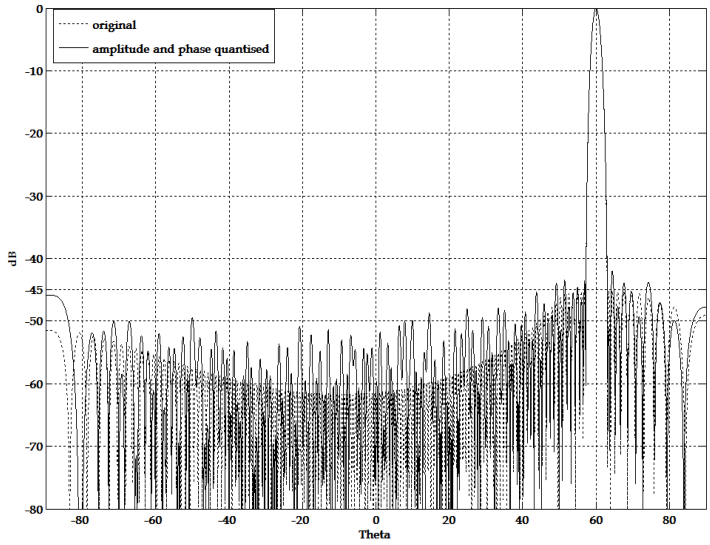


**Figure 4.** Combined effect of 6 bit amplitude and phase quantisations on far-field radiation pattern of $(160 \times 10)$ elements active phased array antenna.

on scanning the radiation pattern in presence of quantisation errors [Figure 4].

### 2.3. Effect of Multilayer Flat Sandwich Radome on the Active Phased Array Antenna Performance

So far a variety of different approaches [2, 10–12] have been employed to investigate the performance of radome-antenna systems. These approaches can be categorised as: 1) High-frequency (HF) methods 2) Low-frequency (LF) methods; and 3) Analytical methods [11]. For some type of radomes having sharp tips such as ogive or cone shaped, low frequency (LF) methods are more accurate but at the cost of extensive computational requirements. However an important assumption of high-frequency (HF) methods is that the structures have smooth surfaces and electrically large radii of curvature. For most realistic airborne radomes this assumption is most valid. Hence HF method has been employed for analysis in the present work.

The analysis of microwave transmission through multilayer flat sandwich radome (FSR) can be achieved via a boundary value solution of the $N$-layer dielectric wall [Figure 5] for forward and reverse propagating waves ($C_i$ and $B_i$, respectively) [2]. *Radome Efficiency* is measured in terms of its transmission capabilities which are measurable from the parameter [2]:

$$T_w = |T_w| \angle \text{IPD} \tag{6}$$

In (6), $T_w$ is the Transmission Coefficient and IPD is Insertion Phase Delay [2]. Radome designers specify the RE in terms of *Radome Transmission Efficiency* (RTE) defined as $|T_w|^2$ [2].

Multilayer Flat Sandwich Radome, with Honeycomb Core [$\varepsilon_{r3} = 1.16$; $t_3 = 1000$ mils (25 mm) typically] and Fiberglass Epoxy Lamination [$\varepsilon_{r2} = 4.25$; $t_2 = 33$ mils (0.84 mm) typically] on either side of the Honeycomb Core, along with a Paint Layer [$\varepsilon_{r1} = 3.65$; $t_1 = 5$ mils (5 mm) typically] has been chosen for analysis [Figure 5a]. A detailed parametric analysis of radome ($f_0 = 3.3$ GHz and bandwidth, BW of 12%) has been presented in our earlier work [13]. The analysis has been carried out for perpendicular (PER) as well as parallel (PAR) polarisations of incident plane wave on the radome surface. Here the results have been reproduced for the sake of continuity.

#### *2.3.1. Multilayer Flat Sandwich Radome Performance w.r.t. Frequency and Angle of Incidence*

Figure 6 shows the variation of RTE and IPD w.r.t. frequency of operation, $f$, for PER as well as PAR polarisation at 0°- and 60°-

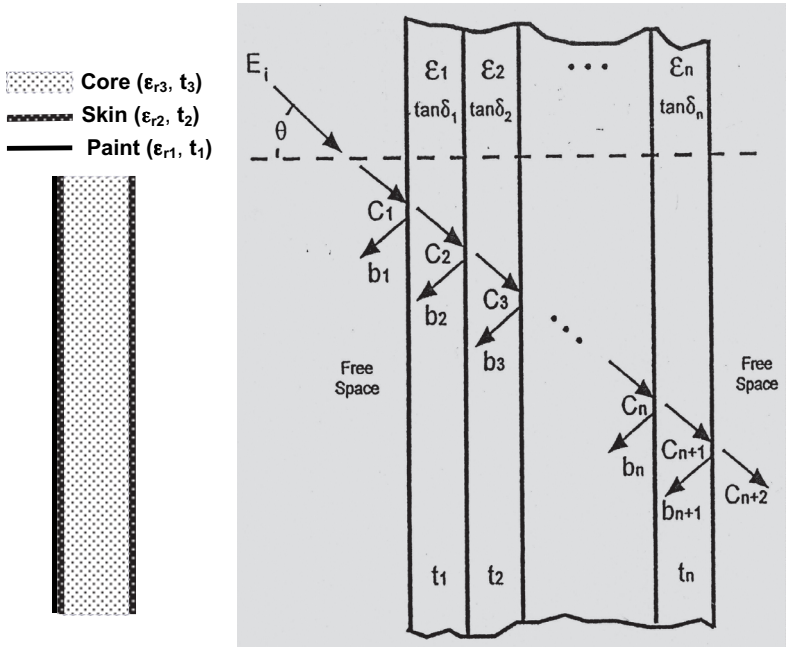


**Figure 5.** Multilayer flat sandwich radome (a). Structural view [$\varepsilon_{r3} = 1.16$; $t_3 = 1000$ mils (25 mm) typically; $\varepsilon_{r2} = 4.25$; $t_2 = 33$ mils (0.84 mm) typically; $\varepsilon_{r1} = 3.65$; $t_1 =$ mils (5 mm) typically] (b). Boundary-value solution of the $N$-layer dielectric wall radome.

angle of incidence of plane wave on the Radome surface. RTE and IPD have shown a decreasing and increasing trend respectively with the increase in $f$. The degradation in RTE and IPD is more for PER as compared to PAR polarisation. Figure 7 shows the decreasing and increasing trend for RTE and IPD w.r.t. angle of incidence for PER and PAR polarisations. Hence it can be inferred that at higher incidences, average of the magnitudes of RTE and IPD for PER and PAR polarisations should be taken in the analysis.

### *2.3.2. Multilayer Flat Sandwich Radome Performance w.r.t. Variation in Constituent Layers of Flat Sandwich Radome*

Detailed discussion of the study of variation of parameters of constituent layers of FSR has been given in our earlier work [13]. Negligible variation has been observed due to variation in

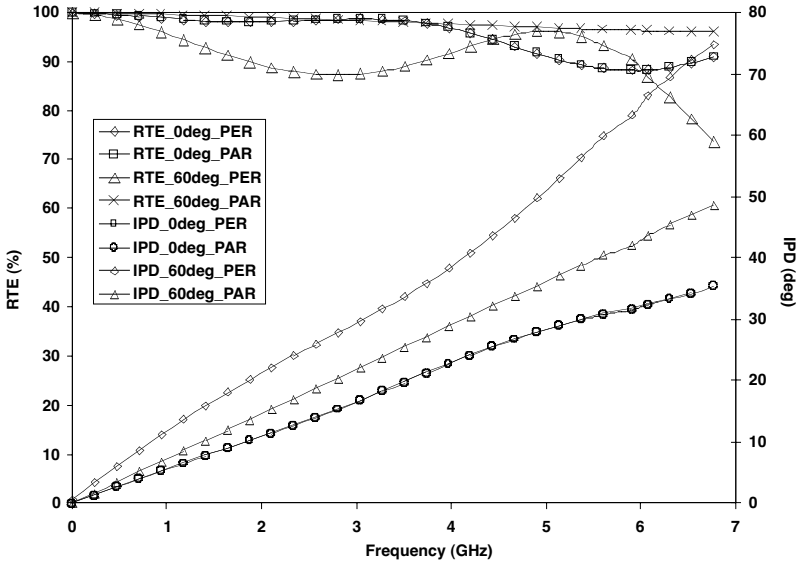


**Figure 6.** Effect of variation in frequency of operation on RTE and IPD of multilayer flat sandwich radome.

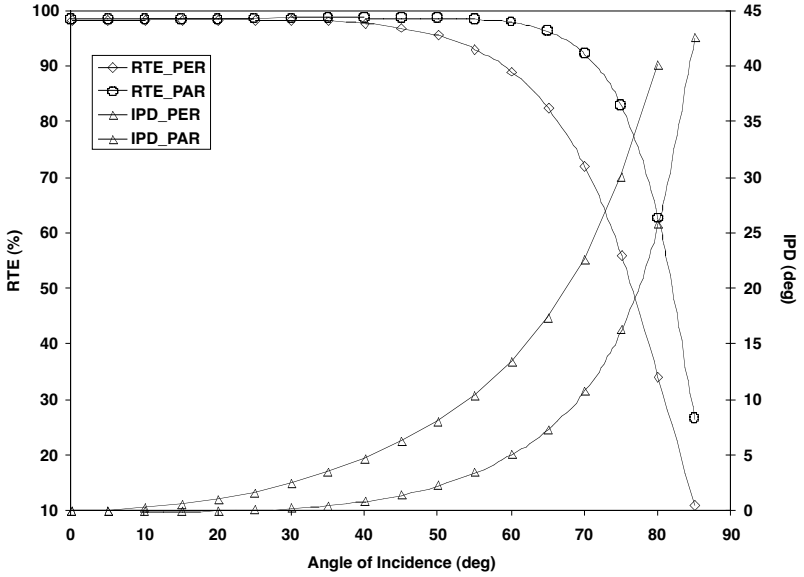


**Figure 7.** Effect of variation in angle of incidence on RTE and IPD of flat sandwich radome.

characteristics of paint layer, hence its effect on array performance has not been considered. The effect of ±5% (10%) variation in the characteristics viz., dielectric constant ($\varepsilon_{r2}$) and the thickness ($t_2$), of lamination layer produces considerable effect on RTE and IPD and hence has been considered in the present analysis. Figure 8 shows the effect of variation in core thickness ($t_3$) of FSR on the RTE and IPD. It can be seen that constraining the variation in $t_3$ within ±2 mm can limit the variation in RTE and IPD to be least even at higher angles of incidence and hence its effect on array performance has been studied. The variations in dielectric constant of core have been neglected as it is close to unity, i.e., that of free space.

### *2.3.3. Active Phased Array Antenna Performance w.r.t. Variation in Core Thickness ($t_3$)*

The variation of ±2 mm (total of 4 mm) in the $t_3$ varies IPD by 1.6° and 2.4° for 0°- and 60°-incidences, respectively [Figure 8]. Introducing phase distortion, $\Lambda = 2°$ (average of 1.6° and 2.4°) in the progressive phase shifts using Eq. (5), degradation in array pattern has been studied [Figure 9]. Degradation in near SLL has been observed to be 0.2 dB to 0.4 dB and on scanning the beam to 60°, degradation is from 0.1 dB to 0.4 dB. However, more degradation has been observed in far SLL on scanning [Figure 10].

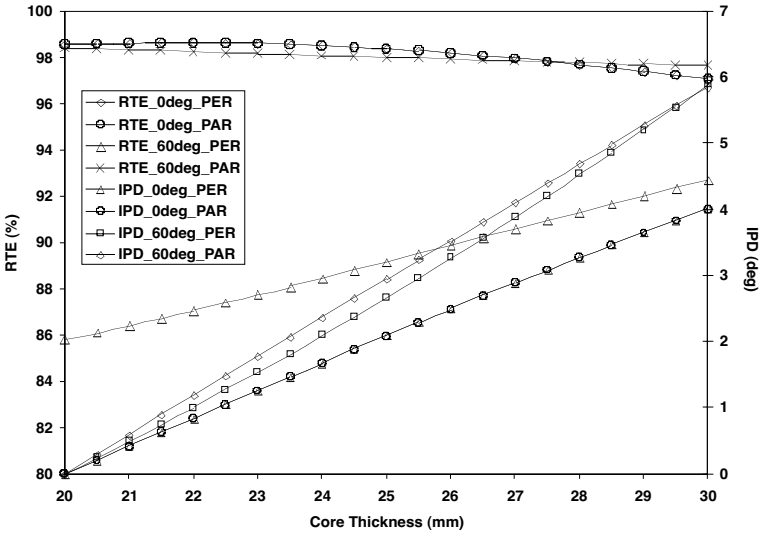


**Figure 8.** Effect of variation in core thickness ($t_3$) of flat sandwich radome on its RTE and IPD.

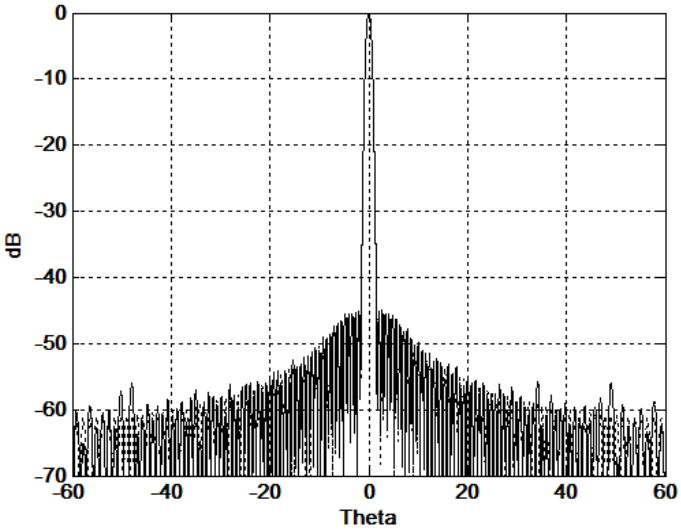


**Figure 9.** Effect of variation in core thickness ($t_3$) of flat sandwich radome on the far field radiation pattern of $(160 \times 10)$ elements active phased array antenna.

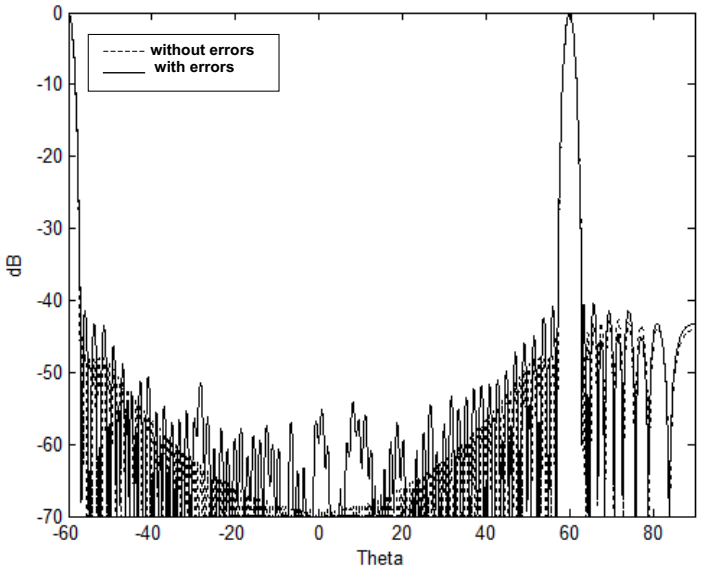


**Figure 10.** Effect of variation in core thickness of flat sandwich radome on the scanned far field pattern of $(160 \times 10)$ elements active phased array antenna.

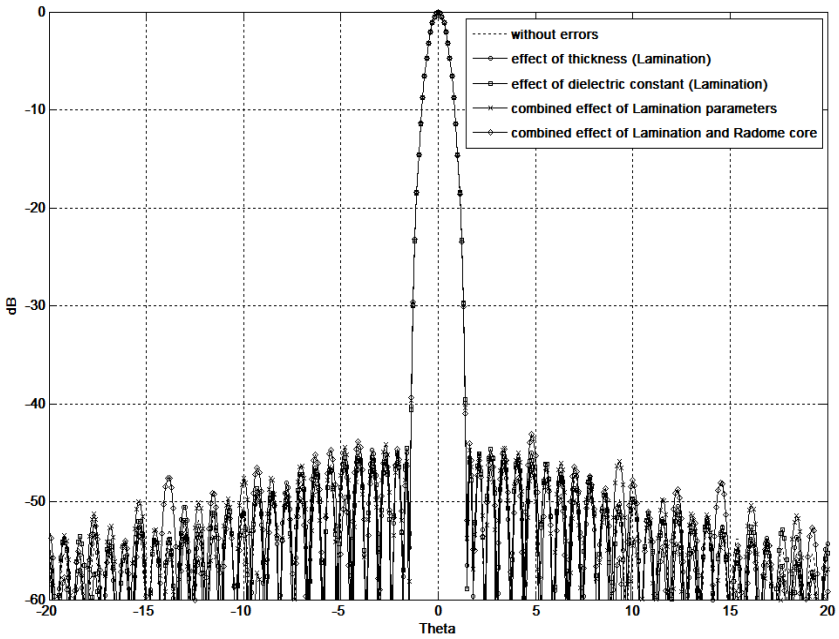


**Figure 11.** Effect of variations in characteristics of lamination layer and core of multilayer flat sandwich radome individually and in combined manner on active phased array antenna radiation pattern.

### *2.3.4. Active Phased Array Antenna Performance w.r.t. Variation in Characteristics of Lamination Layer*

Varying thickness of lamination layer, $t_2$ on either side of core, varies IPD by 1.1° and 1.2° for 0°- and 60°-incidences, respectively. IPD is found to vary by 2.2° and 2.4° for 0°- and 60°-incidences when $t_2$ varies on both sides of core simultaneously [13]. On varying dielectric constant, $\varepsilon_{r2}$, IPD is found to vary by 1.4° and 1.9° for 0°- and 60°-incidences when variation is on either side of the core. Further, IPD varies by 2.8° and 2.7° for 0°- and 60°-incidences, when variation in $\varepsilon_{r2}$ is on both sides of the core [10, 11]. These figures are average of the absolute values for PER and PAR Polarisation cases. The worst case values of phase distortion, ( has been taken to be 2.5° and 3° for 0°- and 60°-incidences, respectively and has been introduced randomly in the array pattern [using Eq. (5)]. Figure 11 has shown a degradation of 0.6 dB and 0.9 dB (max.) in the near SLL.

Next, combined effect of variation in $t_2$ and $_{r2}$ of lamination on the pattern is studied. For this, $\Lambda\sim6°$ [2.5° (due to $t_2$) +3° (due to

$\varepsilon_{r2}$)] has been introduced randomly using Eq. (5), in the progressive phase shifts of active array antenna. A degradation of 1.1 dB (max.) has been observed in the near SLL [Figure 11].

*2.3.5. Active Phased Array Antenna Pattern Performance w.r.t. Combined Effect of Variation in Layers of Flat Sandwich Radome*

Finally, phase distortion, $\Lambda = 8°$, due to combined variation in characteristics of lamination (6°), and variation in Radome core (2°), has been introduced in the progressive phase shifts of the array and its effect on radiation pattern has been studied [Figure 11]. Degradation of 2.6 dB (max.) has been observed in the near SLL along with the little asymmetry in the pattern.

## 2.4. Active Phased Array Antenna Pattern Performance w.r.t Combined Effect of Amplitude/Phase Quantisation Errors, Array Planarity Error and Radome IPD Errors

The effect of Radome IPD errors in conjunction with previous discussed parameters, viz., array planarity, amplitude and phase quantisation errors on the radiation pattern of active phased array antenna has been analysed. Here optimised phase values using Two Probable Value Method have been used. In the analysis, overall phase distortion of 6° [3.96° (due to array planarity error) +2° (IPD variation due to radome core)] has been taken to study degradation of the pattern. A degradation of 0.8 dB to 1.2 dB has been observed in Azimuth Plane. The near side lobe levels rise above −45 B level at few points [Figure 12].

On considering the effect of IPD variation due to variations in characteristics of lamination layer along with the previously discussed errors in last paragraph, $\Lambda = 12°$ [6° (due to AP and core) +6° (lamination)] has been introduced in phase shifts randomly which exhibits a degradation in SLL by ±2 dB [Figure 12]. These errors will be further increased on scanning the beam off boresight. This kind of degradation in SLL can deter the performance of a radar system requiring ultra low sidelobe levels.

Further, considering only ±1 mm (total of 2 mm) and ±0.5 mm (total of 1 mm) variation in thickness of Radome core, producing IPD variations of 0.7° and 0.4° [Figure 8], respectively, have been combined with phase distortions due to lamination and array planarity and introduced in the progressive phase shifts of the array using Eq. (5). The combined degradation has been observed to be least, less than 0.9 dB, for ±0.5 mm (total of 1 mm) tolerance in thickness of Radome core as compared to the other cases [Figure 12].

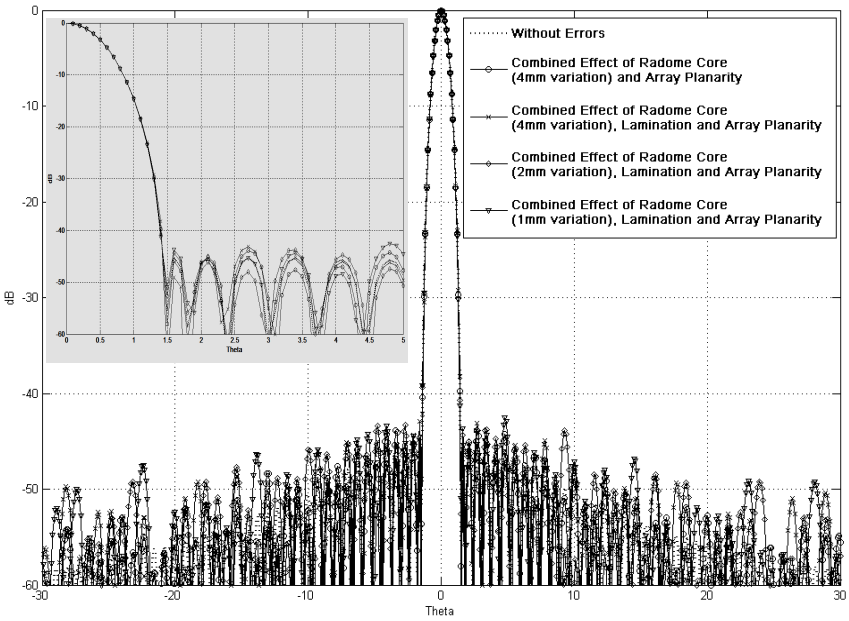


**Figure 12.** Combined effect of variations in characteristics of multilayer flat sandwich radome (with different core thickness), 6 bit amplitude/phase quantisation error and array planarity error on active phased array antenna radiation pattern (exploded view of one half of the pattern is shown as an inset).

## 3. CONCLUSION

A detailed study of degradation of active phased array antenna radiation characteristics due to amplitude and phase quantisation errors, array planarity error combined with the errors due to IPD variations as a result of variations in the thickness and dielectric constant of the various layers of the multilayer flat sandwich radome has been presented in this paper. It has been shown that by constraining the manufacturing tolerances of radome, viz., variation in radome core less than $\pm 1$ mm (total of 2 mm), preferably $\pm 0.5$ mm (total of 1 mm), and variation in characteristics of lamination layer less than 10% ($\pm 5\%$), preferably 5% ($\pm 2.5\%$), can reduce the array pattern degradation in terms of sidelobe level within tolerable limits. This work is expected to be useful in appraising a radome to be qualified for its usage in various active phased array radars and other similar applications where ultra low sidelobe levels are desired.

## REFERENCES


1. Williams, F. C. and M. E. Radant, "Airborne radars and the three PRFs," *Microwave Journal*, 129–135, 1983.
2. Kozakoff, D. J., *Analysis of Radome-Enclosed Antennas*, Artech House, 1997.
3. Skolnik, M. I., *Non-uniform Arrays*, R. E. Collin and F. J. Zucker (eds.), Ch. 6, 227–234, McGraw-Hill, New York, 1969.
4. Steinberg, B. D., *Principles of Aperture and Array Systems Design*, John Wiley and Sons, New York, 1976.
5. Mailloux, R. J., *Phased Array Antenna Handbook*, Artech House, 2005.
6. Miller, C. J., "Minimizing the effects of phase quantization errors in an electronically scanned array," *Proc. 1964 Symp. Electronically Scanned Phased Arrays and Applications, RADC-TDR-64-225, RADC Griffiss AFB*, 17–38, 1964.
7. Brookner, E., *Practical Phased Array Antenna Systems*, Artech House, 1991.
8. Smith, M. S. and Y. C. Guo, "A comparison of methods for randomising phase quantisation errors in phased arrays," *IEEE Trans Antennas and Propagat.*, 6–12, 1983.
9. Revankar, U. K., K. S. Beenamole, K. Sreenivasulu, and K. M. Veerabhadra, "Sidelobe minimisation in active phased arrays," *IETE Tech. Review*, 191–196, 2001.
10. Li, L.-W., L. Zhou, M. S. Leong, T.-S. Yeo, and P. S. Kooi, "An open-ended circular waveguide with an infinite conducting flange covered by a dielectric hemi-spherical radome shell: Full-wave analysis and Green dyadics," *Progress In Electromagnetics Research*, PIER 21, 221–245, 1999.
11. Li, L.-W. and W.-X. Zhang, "Electromagnetic scattering of a thin circular loop enclosed by a spherical chiral radome shell: A method of moments analysis," *Progress In Electromagnetics Research*, PIER 35, 141–163, 2002.
12. Nie, X.-C., N. Yuan, L.-W. Li, T.-S. Yeo, and Y.-B. Gan, "Fast analysis of electromagnetic transmission through arbitrary shaped airborne radomes using precorrected-FFT method," *Progress In Electromagnetics Research*, PIER 54, 37–59, 2005.
13. Revankar, U. K., A. Kedar, V. Saravana Kumar, and K. S. Beenamole, "Effect of thickness variation of flat sandwich radome on array pattern performance in S-band," *Int. Radar Symp. India*, Bangalore, India, 2005.